Understanding Crack Size Effects during Fatigue of Extrinsically Toughened Materials

J. J. Kruzic[1]
Oregon State University, Corvallis, OR, USA

Abstract

Despite more than two decades of research on the topic, there are currently few practical tools for incorporating crack size (i.e., small or short crack) effects into fatigue life predictions in real engineering applications. This paper examines how fatigue resistance curves (fatigue *R*-curves or fatigue threshold *R*-curves) may be used to understand and predict such crack size effects. Recently published and new experimental fatigue *R*-curve results are presented for human bone and polycrystalline Al_2O_3. When fatigue crack growth resistance is plotted as a function of crack size on *R*-curves, clear trends of increasing with crack extension are seen for both materials. Also, when those crack size effects arise from extrinsic toughening mechanisms, like crack bridging in Al_2O_3, it is demonstrated that the fatigue behavior at all crack sizes can be predicted by carefully characterizing the bridging zone and quantifying the effects of bridging using only long crack experiments. Experimentally measured short crack fatigue threshold data agrees well with the predictions based on quantitative bridging zone characterization. Finally, as with fracture *R*-curves, it is shown that there is a strong effect of microstructure on the fatigue threshold *R*-curve shape, which in turn is expected to affect the fatigue strength of the material.

1. Introduction

A major unresolved issue in modern fatigue analysis is that of crack size effects, also termed short or small crack effects. Short cracks can behave quite differently from longer cracks, in particular by exhibiting fatigue-crack growth rates that far exceed those of corresponding long cracks subjected to the same applied driving force and also by propagating at ΔK levels *less than* the fatigue threshold, ΔK^{TH}, below which long cracks are presumed to be dormant [3-7]. Although crack size effects have been recognized as problems in the fatigue of materials for more than two decades, in that time little progress has been made in quantitatively incorporating such phenomena into rational tools for making reliability predictions that are suitable for engineering design purposes. Most research efforts over that time have focused on characterizing the growth rates of short fatigue cracks in specific materials, which has proven to be i) experimentally difficult and in some cases intractable, ii) costly and time consuming, and iii) has yielded widely scattered data which cannot be utilized in traditional damage tolerant fatigue life predictions.

[1] Corresponding author. Tel: +1-541-737-7027; fax: +1-541-737-2600.
E-mail address: jamie.kruzic@oregonstate.edu (J. J. Kruzic)

Crack size effects in fatigue are widely observed in metals [3,5,6], ceramics [2,8], intermetallics [9,10], composites, and biological materials [1,11] where crack sizes are comparable to, or less than, one of three characteristic dimensions, namely, that of the microstructure, the extent of local inelasticity (i.e., plastic-zone size) *ahead* of the crack tip, and/or the extent of the zone causing crack-tip shielding or bridging (i.e., extrinsic toughening) *behind* the crack tip. The present paper will focus on recent efforts to incorporate crack size effects into a damage tolerant methodology utilizing the fatigue threshold *R*-curve approach, as well as how to make accurate predictions of short crack behavior in extrinsically toughened materials with relatively few carefully designed experiments.

2. Fatigue resistance curves (*R*-curves)

One challenge to understanding crack size effects is the large amount of scatter in crack growth rates for small cracks when plotted on traditional crack growth rate, *da/dN or dc/dN*, versus stress intensity range, ΔK, plots. Fig. 1a shows an example for human cortical bone, where surface cracks smaller than ~1 mm in total length show characteristic small crack behavior due to crack bridging [1]. Specifically, the small crack data is highly scattered with 1) faster crack growth at a given ΔK level and 2) growth occurring below the long crack threshold. Such highly scattered data is typical of the small crack fatigue literature for a variety of materials; however, if one re-plots the data as a function of crack size using a fatigue resistance curve (Fig. 1b), a clear trend in the short crack behavior is seen. The fatigue *R*-curve is analogous to the well known fracture *R*-curve, with the added requirement that the data only be plotted for a single crack growth rate (or

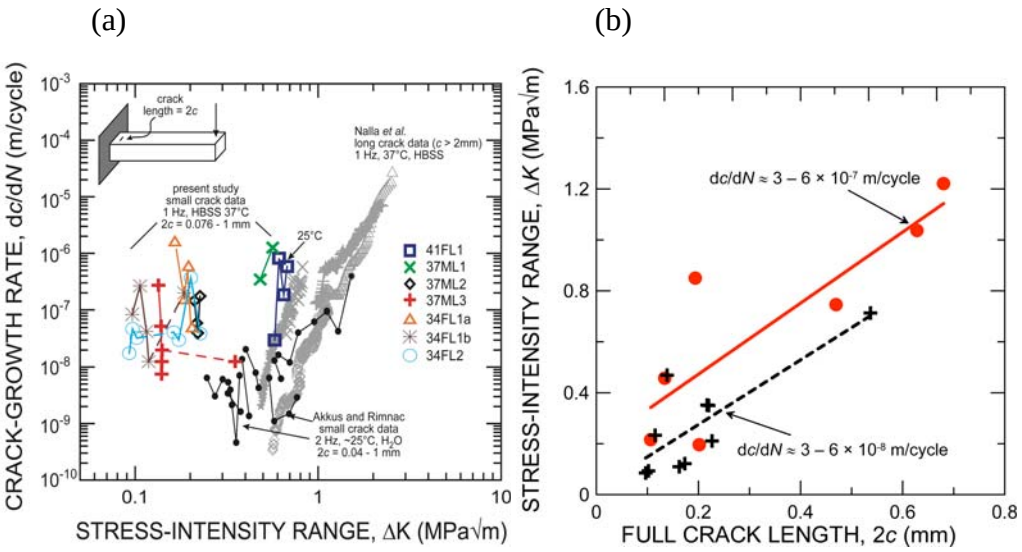

Fig. 1. Small crack data for human cortical bone is plotted in (a) as a traditional *dc/dN*-ΔK curve while in (b) some of the same data is plotted as fatigue resistance curves for specific growth rates. Figures reproduced from with permission from [1]

tight range) to allow fair comparison. In Fig. 1b, a clear trend of increasing fatigue resistance is seen with crack extension, as may be expected based on the rising fracture resistance that is also seen in bone [12]. The fatigue *R*-curve allows a clear representation of the variation in fatigue resistance with crack size.

3. Fatigue threshold *R*-curves

By plotting the fatigue *R*-curve for growth rates corresponding to the fatigue threshold, which is often operationally defined as growth on the order of 10^{-10} m/cycle, one gets a fatigue threshold *R*-curve [2,13,14]. Fig. 2a shows a fatigue threshold *R*-curve plotted for a 99.5% pure Al_2O_3 ceramic [2]. In Fig. 2a, the round data points represent actual measured fatigue thresholds (25 Hz sine wave, load ratio, $R = 0.1$) plotted in terms of the maximum stress intensity during the lading cycle, K_{max}. By plotting in terms of K_{max}, the *R*-curve can be assumed to begin at zero crack extension, $\Delta a = 0$, at the intrinsic toughness of the material, K_0. Data is given for short cracks in multiple compact tension, C(T), specimens ($W \approx 17$ mm, $B \approx 3$mm) tested in ambient room air. A clear trend of increasing fatigue threshold may be seen over the first 2 mm of crack extension, a length which corresponds to the observed transition from short to long crack behavior in this alumina [8].

Also shown in Fig. 2a is the fatigue threshold *R*-curve predicted based on independent measurements of the bridging stresses for a long fatigue crack in that same alumina (Fig. 2b). The bridging stresses were estimated using a combination of crack opening displacement measurements and multi-cutting compliance experiments, complete details may be found in Ref. [8]. The contribution of bridging, K_{br}, was deduced by integrating the bridging stress distribution, $\sigma_{br}(x)$, using the weight function approach [15]:

$$K_{br} = \int_0^a h(x,a)\sigma_{br}(x)dx, \qquad (1)$$

where x is the position along the crack measured from the load line and the weight function, h, is geometry specific and may be found for the C(T) specimen in ref. [16]. In the present case, $\sigma_{br}(x)$ represents the bridging stress distribution for a long crack held at K_{max} after being grown near the long crack fatigue threshold. Through the use of Eq. 1, the near-threshold bridging contributions, $K_{br}(\Delta a)$ for any amount of crack extension, Δa, may be deduced, allowing the prediction of a fatigue threshold *R*-curve via:

$$K_{max}^{TH}(\Delta a) = K_0 + K_{br}(\Delta a), \qquad (2)$$

where K_0 is simply the intrinsic resistance to crack propagation, or intrinsic toughness, of the material, which has been determined to be ~1.3 - 1.4 MPa$\sqrt{m}$ for this alumina [8,17].

It is important to note that the predicted fatigue threshold is based solely on measurements of the fatigue behavior of long cracks and by deducing the bridging

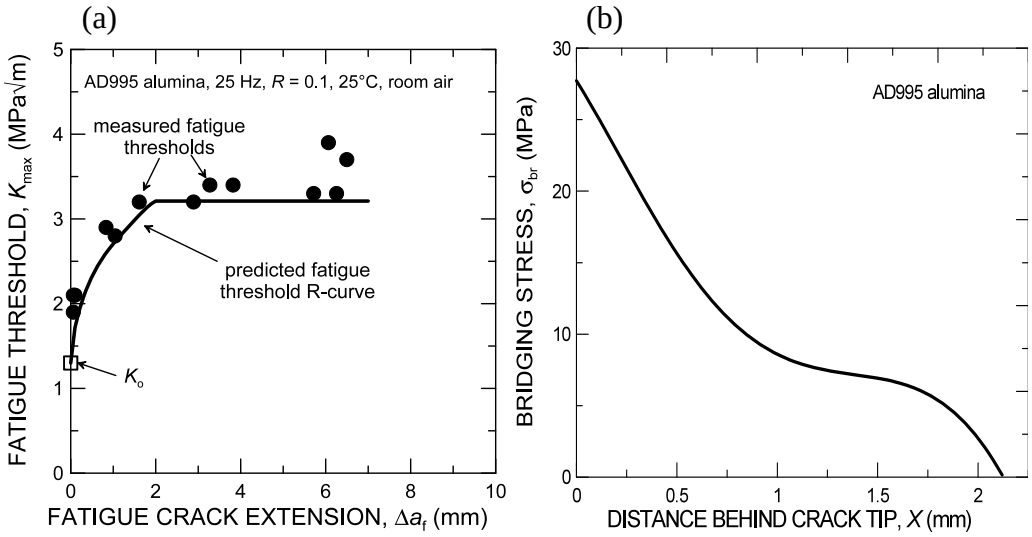

Fig. 2. In (a), the measured fatigue threshold R-curve data points are potted along with the predicted curve based on the bridging stress distribution shown in (b) by using Eqs. 1 & 2. Figures reproduced with permission from [2].

stress distribution of those cracks, thereby eliminating the need for difficult and costly short crack experiments. This is a powerful tool for predicting the crack size effects in materials extrinsically toughened by crack bridging.

4. Role of microstructure

In ceramics toughened by grain bridging, it is well known that several microstructural parameters can affect the fracture *R*-curve, including grain size, shape, size distribution and boundary adhesion. It should be expected that fatigue threshold *R*-curves will be similarly effected by these factors; however, currently there is very little experimental data. With regard to the latter factor, recent studies on the fracture behavior have shown that the optimal window for grain boundary adhesion is small; if the boundaries are too strong, transgranular fracture leads to low toughness and strength, but when boundaries are too weak, the fracture *R*-curve rises slowly, giving lower toughness, strength, and fatigue resistance [17,18]. The current section describes new results on the role of grain boundary adhesion in affecting the fatigue threshold *R*-curve.

4.1. Materials

The same commercial 99.5% pure alumina (AD995, Coors Technical Ceramics Co., Oak Ridge, TN) described above was examined in this study. This alumina has a wide grain size distribution, with a mean lineal intercept of 12 μm. If one assumes the grains to be equiaxed and equal in size, that would give an average grain diameter of ~18 μm; however, as there was in fact a wide distribution of grain diameters more information on the material microstructure may be found in Ref. [8].

4.2. Fatigue threshold experiments

Fatigue-crack growth experiments were conducted on standard compact-tension, C(T), specimens (width, $W \approx 17$ mm; thickness, $B \approx 3 - 3.5$ mm) in general accordance with ASTM standard E647 [19]. Complete details of the fatigue-crack growth procedures are in Ref. [8]; a brief summary of issues pertinent to the measurement of fatigue thresholds is presented here. Fatigue cracks were initiated from straight machined notches (length $a_o \approx 4 - 5$ mm) under cyclic loading conditions (25 Hz sine wave, load ratio, $R = 0.1$), after which the cracks were grown to a specified length, as monitored using back-face strain compliance methods [20]. Notch root radii, ρ, ranged from ~15 – 150 μm, with the sharpest notches used for the smallest crack sizes. In all cases, data collection did not begin until the amount of fatigue-crack extension from the notch, Δa_f, exceeded ρ, at which point the influence of the notch field on the stress intensity could be considered to be negligible [21,22]. In order to measure the fatigue threshold, the applied stress-intensity range was reduced at a roughly constant ΔK-gradient (= $[d\Delta K/da] /\Delta K$) of -0.08 mm^{-1}. In such manner, the fatigue threshold was measured as a function of crack extension for Δa_f ranging from 60 μm to 8.8 mm, with the threshold operationally defined as the lowest stress intensity at which the fatigue-crack growth rate was ~10^{-10} m/cycle.

4.3. Testing Environments

The ascertain the effects of changing grain boundary adhesion, fatigue threshold data is compared from tests conducted at 25ºC in i) moist room air with relative humidity of ~20 to 50% (Fig. 2a) and ii) flowing dried nitrogen gas. This approach was used because fatigue cracks propagate predominantly along the glassy grain boundary phase, and it is well known that the presence of moisture serves to lower the intrinsic resistance to crack advance in silicate glasses at sub-critical velocities [23-25]. Thus, by testing in a dry environment one is able to study two different levels of grain boundary adhesion without any changes in microstructure. 99.999% pure N_2 was passed through a commercial purifier (Gatekeeper, Aeronex, San Diego, CA) rated to purify to sub parts per billion (ppb) levels of moisture, and then through a carefully baked out stainless steel and aluminum testing chamber. Full details on the test chamber bake-out and gas drying procedures are reported elsewhere, and in that study the H_2O content of the nitrogen gas was estimated to be < 50 ppb [17].

4.4. Results

Fig. 3a shows a comparison of the fatigue threshold R-curves for AD995 alumina in both the dry and moist environments potted in terms of $K_{max}(\Delta a)$. The moist air environment data was also presented in Fig. 2 and is from a previous study [2]. Values of K_0 were taken from a previous study to be 1.4 MPa$\sqrt{m}$ for the most air

case, and 2.0 MPa√m for the dry nitrogen case [17]. From Fig. 3a, it is clear the fatigue threshold *R*-curve rises more steeply for the dry nitrogen case where the grain boundaries are not weakened by moisture. Such behavior is analogous to what is seen in the fracture *R*-curves, where the tougher grain boundaries associated with the inert environment lead to steeper *R*-curves and higher strength [17].

5. Fatigue strength predictions

In situations using high frequency loading or materials with high Paris law exponents (ceramics, some intermetallics and composites), the time to fatigue failure will be short once cracks begin to grow, which provides motivation for reliability predictions based on fatigue thresholds. An attractive property of fatigue threshold *R*-curves is the potential ability to predict fatigue endurance strengths, i.e., the stress level below which the material should be immune to fatigue failure, based on the size of the largest initial flaw in a component. Based on the methods of fracture *R*-curves to determine the fracture strength, it follows that the fatigue limit, or endurance strength, for an internal penny shaped flaw may be predicted from the fatigue threshold *R*-curve:

$$\Delta K_{app} = 2\Delta\sigma_{app}\sqrt{\frac{\Delta a + a_i}{\pi}} = \Delta K_{TH}(\Delta a) \qquad (3a)$$

$$\frac{d\Delta K_{app}}{d\Delta a} = \frac{d\Delta K_{TH}(\Delta a)}{d\Delta a} \qquad (3b)$$

where $\Delta\sigma_{app}$ is the applied stress range. Such a methodology should be useful for both experimentally determined fatigue threshold *R*-curves, which would include any type of crack size effect due to microstructure, plasticity, or extrinsic toughening, as well as those predicted using the distribution of bridging stresses, as was described above.

Using the fatigue threshold *R*-curves seen in Fig. 3a, Eq. 3 was applied to calculate the expected fatigue strength as a function of initial flaw radius for a penny shaped flaw and a load ratio of $R = 0.1$. These predictions are shown in Fig. 3b, showing the higher expected fatigue strength in the dry environment. It is reasonable that the fatigue strength would be higher in the dry environment considering that the fracture strength of this and other alumina ceramics as known to be degraded by humidity [26-31], which can be attributed to changes in the grain boundary adhesion and the fracture resistance curve behavior [17].

6. Conclusions

1) The fatigue *R*-curve provides a rational way to present the effect of crack size on the fatigue crack growth behavior as a singe growth rate or tight growth rate range.

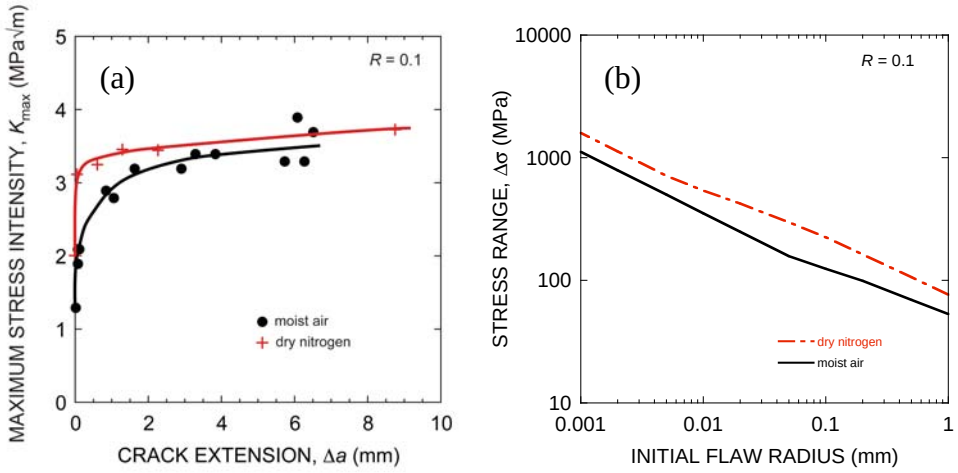

Fig. 3. Results for a 99.5% pure alumina in moist air and dry nitrogen illustrating how enhanced grain boundary adhesion leads to (a) a steeper fatigue threshold *R*-curve and (b) higher expected fatigue strengths.

2) By defining the growth rate essentially at the fatigue threshold (~10^{-10} m/cycle), a fatigue threshold *R*-curve may be obtained.

3) Fatigue threshold *R*-curves can be useful for predicting the fatigue strength of materials analogous to the way fracture *R*-curves are used to predict fracture strength of materials.

4) Finally, when crack size effects are due to extrinsic toughening, such as crack bridging, the fatigue threshold *R*-curve can be predicted by quantifying the shielding stresses, potentially eliminating the need for costly and time consuming short crack experiments.

Acknowledgements

The author would like to acknowledge financial support from the National Science Foundation CAREER Award No. 0547394 as well as numerous useful discussions with Dr. Rowland M. Cannon.

References

[1] J.J. Kruzic, J.A. Scott, R.K. Nalla, R.O. Ritchie, Propagation of surface fatigue cracks in human cortical bone, J Biomech 38 (5) (2006) 968-972
[2] J.J. Kruzic, R.M. Cannon, J.W. Ager III, R.O. Ritchie, Fatigue threshold R-curves for predicting reliability of ceramics under cyclic loading, Acta Mater 53 (9) (2005) 2595-2605
[3] K.J. Miller, The short crack problem, Fatigue Eng Mater Struct 5 (1982) 223-232

[4] R.O. Ritchie, S. Suresh, The fracture mechanics similitude concept: questions concerning its application to the behavior of short fatigue cracks, Mater Sci Eng 57 (2) (1983) L27-L30
[5] S. Suresh, R.O. Ritchie, Propagation of short fatigue cracks, Int Metals Rev 29 (6) (1984) 445-476
[6] R.O. Ritchie, J. Lankford, Small fatigue cracks: a statement of the problem and potential solutions, Mater Sci Eng A84 (1986) 11-16
[7] R.O. Ritchie, W. Yu. Short crack effects in fatigue: a consequence of crack tip shielding, in: R.O. Ritchie, J. Lankford (Eds.), Small Fatigue Cracks, TMS-AIME, Warrendale, PA, 1986, pp. 167-189
[8] J.J. Kruzic, R.M. Cannon, R.O. Ritchie, Crack size effects on cyclic and monotonic crack growth in polycrystalline alumina: Quantification of the role of grain bridging, J Am Ceram Soc 87 (1) (2004) 93-103
[9] J.P. Campbell, J.J. Kruzic, S. Lillibridge, K.T. Venkateswara Rao, R.O. Ritchie, On the growth of small fatigue cracks in γ-based titanium aluminides, Scripta Mater 37 (5) (1997) 707-712
[10] J.J. Kruzic, J.P. Campbell, R.O. Ritchie, On the fatigue behavior of γ-based titanium aluminides: Role of small cracks, Acta Mater 47 (3) (1999) 801-816
[11] O. Akkus, C.M. Rimnac, Cortical bone tissue resists fatigue fracture by deceleration and arrest of microcrack growth, J Biomech 34 (6) (2001) 757-764
[12] R.K. Nalla, J.J. Kruzic, J.H. Kinney, R.O. Ritchie, Mechanistic aspects of fracture and R-curve behavior of human cortical bone, Biomaterials 26 (2) (2005) 217-231
[13] R. Pippan, M. Berger, H.P. Stüwe, The influence of crack length on fatigue crack growth in deep sharp notches, Metall Trans 18A (1987) 429-435
[14] K. Tanaka, Y. Akiniwa, Resistance-curve method for predicting propagation threshold of short fatigue cracks at notches, Eng Fract Mech 30 (6) (1988) 863-876
[15] H.F. Bueckner, A novel principle for the computation of stress intensity factors, Z Angew Math Mech 50 (9) (1970) 529-546
[16] T. Fett, D. Munz, Stress Intensity Factors and Weight Functions, Computational Mechanics Publications, Southampton, UK, 1997
[17] J.J. Kruzic, R.M. Cannon, R.O. Ritchie, Effects of moisture on grain-boundary strength, fracture and fatigue properties of alumina, J Am Ceram Soc 88 (8) (2005) 2236-2245
[18] J.J. Kruzic, R. Satet, M.J. Hoffmann, R.M. Cannon, R.O. Ritchie, The utility of R-curves for understanding fracture toughness-strength relations in bridging ceramics, J Am Ceram Soc 91 (6) (2008) 1986-1994
[19] ASTM E647-00, in: Annual Book of ASTM Standards, Vol 0301: Metals-Mechanical Testing; Elevated and Low-temperature Tests; Metallography, ASTM International, West Conshohocken, Pennsylvania, USA, 2004, pp. 595-635
[20] W.F. Deans, C.E. Richards, A simple and sensitive method of monitoring crack and load in compact fracture mechanics specimens using strain gages, J Test Eval 7 (3) (1979) 147-154
[21] N.E. Dowling, Notched member fatigue life predictions combining crack initiation and propagation, Fatigue Eng Mater Struct 2 (1979) 129-138

[22] A.N. Palazotto, J.G. Mercer, Crack considerations in a notched compact tension specimen, Eng Fract Mech 37 (3) (1990) 473-492
[23] S.M. Wiederhorn, Influence of water vapor on crack propagation in soda-lime glass, J Am Ceram Soc 50 (8) (1967) 407-414
[24] S.M. Wiederhorn, Moisture assisted crack growth in ceramics, Int J Fract Mech 4 (2) (1968) 171-177
[25] T.A. Michalske, S.W. Freiman, A molecular mechanism for stress corrosion in vitreous silica, J Am Ceram Soc 66 (4) (1983) 284-288
[26] G.K. Bansal, W.H. Duckworth, D.E. Niesz, Strength-size relations in ceramic materials: Investigation of an alumina ceramic, J Am Ceram Soc 59 (11-12) (1976) 472-478
[27] S.-J. Cho, K.-J. Yoon, J.-J. Kim, K.-H. Kim, Influence of humidity on the flexural strength of alumina, J Eur Ceram Soc 20 (6) (2000) 761-764
[28] S.-J. Cho, K.-J. Yoon, Y.-C. Lee, M.-C. Chu, Effects of environmental temperature and humidity on the flexural strength of alumina and measurement of environment-insensitive inherent strength, Mater Lett 57 (18) (2003) 2751-2754
[29] C.C. McMahon, Relative humidity and modulus of rupture, Am Ceram Soc Bull 58 (9) (1979) 873
[30] A.G. Evans, A method for evaluating the time-dependent failure characteristics of brittle materials - and its application to polycrystalline alumina, J Mater Sci 7 (1972) 1137-1146
[31] S. Lathabai, B.R. Lawn, Fatigue limits in noncyclic loading of ceramics with crack-resistance curves, J Mater Sci 24 (12) (1989) 4298-4306